

## Measurement of the Rotational Transform at the Axis of a Tokamak

W. P. West, D. M. Thomas, and J. S. deGrassie  
*GA Technologies Inc., San Diego, California 92138*

and

S. B. Zheng<sup>(a)</sup>  
*Fusion Research Center, University of Texas, Austin, Texas 78712*  
 (Received 15 December 1986)

Measurements of the internal magnetic field structure of Texas Experimental Tokamak discharges are made by use of laser-induced fluorescence of an injected Li<sup>0</sup> beam. From measurements near the magnetic axis, we obtain the axial safety factor,  $q_0$  (or equivalently the rotational transform,  $\iota=2\pi/q$ ) for various discharge conditions. In particular, for low- $q_a$  sawtooth discharges, we find time-averaged values of  $q_0$  significantly less than 1 ( $\approx 0.7$  to 0.8), in contrast with models used to describe the nonlinear internal relaxation process commonly known as sawteeth.

PACS numbers: 52.55.Fa, 52.30.Bt, 52.70.Ds

The safety factor  $q$ , related to the rotational transform  $\iota$ , of the magnetic field in a tokamak by  $q=2\pi/\iota$ , is of prime importance to the stability and confinement of the plasma.<sup>1</sup> However, there have been few direct measurements of  $q$  within the plasma of a tokamak.<sup>2-5</sup> Most of the theoretical models of the  $q$  profile predict that the  $q=1$  surface within the plasma is MHD unstable to kink perturbations. The nonlinear evolution of this instability appears to be responsible for an oscillation of the core temperature known as sawteeth.<sup>6-8</sup> Theory indicates that this relaxation oscillation tends to keep  $q$  near the axis close to unity.<sup>8</sup> In contrast, recent measurements of the Faraday rotation of far-infrared laser radiation on the TEXTOR device at the Institut für Plasmaphysik, Jülich,<sup>7</sup> have indicated that  $q$  near the central axis,  $q_0$ , can be significantly less than 1, e.g.,  $q_0=0.7$ . However, the Faraday-rotation technique requires two sequential Abel inversions to obtain the result, giving rise to some uncertainty in the interpretation.

Here, we report a measurement of the tilt of the magnetic field at the equatorial plane of the Texas Experimental Tokamak<sup>9</sup> (TEXT) at several radial positions using laser-induced fluorescence of an injected neutral Li beam. For small minor radius of a magnetic surface,  $r$ , the safety factor  $q$  can be accurately approximated by

$$q(r) = r/R\theta_1, \quad (1)$$

where  $R$  is the major radius of the magnetic axis. The angle  $\theta_1$ , the tilt of the magnetic field at  $r$ , is given by

$$\theta_1(r) = \arctan[B_p(r)/B_t(r)], \quad (2)$$

where  $B_p(r)$  [ $B_t(r)$ ] is the poloidal (toroidal) magnetic field at  $r$ . In the equatorial plane,  $B_p$  is a vertical magnetic field. As  $r \rightarrow 0$ ,  $B_p \propto rj_0$ , is the current density on axis, and  $q$  becomes independent of  $r$ . So near the axis,

$\theta_1(r)$  is linear and

$$q_0 = 1/R(d\theta_1/dr)_0, \quad (3)$$

where  $(d\theta_1/dr)_0$  is evaluated at the axis. Since the diagnostic system used here measures  $\theta_1$  at several radial positions near  $r=0$ , it is a simple matter to determine  $q_0$  from Eq. (3).

The angle  $\theta$  is measured by use of laser-induced fluorescence of the  $\pi$  component of the Zeeman-split Lorentz triplet of neutral lithium. The diagnostic system has been described in detail elsewhere<sup>10-12</sup> and will be briefly reviewed here. The complete system consists of a neutral Li beam injector, a cw dye laser, a nine-channel optical detection unit, and data-acquisition and -analysis electronics. The dye laser is directed collinearly with the neutral Li beam into the plasma through the central axis of the tokamak in the plane of the equator. The dye laser has a bandwidth of  $\approx 1$  GHz and is tuned into resonance with the  $\pi$  line of the  $2S-2P$  Lorentz triplet (the magnetic fields in TEXT are  $> 1.2$  T, resulting in the Zeeman splitting being driven into the Paschen-Back regime). A set of three collection lenses focuses the fluorescence from the Li beam induced by the laser and by collisions with the plasma species onto a set of nine fiber-optic bundles. Each bundle directs the light through a collimating lens, a 10-Å-bandwidth interference filter, and a focusing lens, and onto a photomultiplier tube.

Before the laser beam is merged with the Li beam, it is passed through a LiNbO<sub>3</sub> polarization rotator, resulting in an electric field vector which has the form

$$\mathbf{E}(r,t) = E_0 \cos \omega_L t (\hat{\mathbf{x}} \cos \omega_m t + \hat{\mathbf{y}} \sin \omega_m t), \quad (4)$$

where  $\omega_L$  is the frequency of the light, and  $\omega_m/2\pi=50$  kHz is the polarization rotation frequency. Since the  $\pi$

line is linearly polarized parallel to the local magnetic field direction, the rate of laser excitation is given by

$$R_L(r,t) = f[\hat{\mathbf{E}} \cdot \hat{\mathbf{B}}]^2 \sigma_L I_L / h\nu, \quad (5)$$

where  $\hat{\mathbf{E}}$  and  $\hat{\mathbf{B}}$  are unit vectors in the direction of the laser-light electric field and the local magnetic field, respectively;  $\sigma_L$  is the photoexcitation cross section,  $I_L$  is the laser beam intensity at photon energy  $h\nu$ , and  $f$  is a form factor related to the spatial and spectral overlaps of the laser and Li beams. The laser-induced fluorescence signal detected by a single channel of the optical detection unit viewing the beam at radius  $r$  is given by

$$S_L(r,t) = A' \{1 + \cos 2[\omega_m t + \theta_1(r,t) - \theta_\tau(r,t) + \Delta\theta(r,t)]\}, \quad (6)$$

where  $A'$  includes all the time-independent factors. The phase shift  $\theta_1(r,t)$  results from the tilt of the magnetic field [see Eq. (2)]. Since the Li 2P state has finite lifetime  $\tau$ , a phase delay  $\theta_\tau(r,t)$  results from the delay for reradiation, where

$$\theta_\tau = \tau \omega_m. \quad (7)$$

Note that because of collisional effects,  $\tau$  is a function of local plasma density. In the absence of collisions,  $\tau = 27$  ns. A phase shift  $\Delta\theta(r,t)$  results from the finite lifetime and the variation of  $\theta_1$  with radius<sup>12</sup>:

$$\Delta\theta = u\tau d\theta_1/dr, \quad (8)$$

where  $u$  is the velocity of the Li atoms ( $1.8 \times 10^8$  cm/s).

Quadrature demodulation at  $\omega_m$  allows the total phase shift  $\theta_m$  of each detected signal with respect to a reference signal to be determined:

$$\theta_m(r,t) = \theta_1(r,t) - \theta_\tau(r,t) + \Delta\theta(r,t). \quad (9)$$

The measured phase shift near the magnetic axis as a function of time during a tokamak discharge is shown in Fig. 1 along with the plasma current, line-averaged electron density, horizontal plasma position, and the central-chord soft x-ray signal. On each discharge the toroidal field is ramped up and flat-topped a few hundred milliseconds before  $t=0$  (discharge initiation), providing a zero reference for phase. Since the measured phase shown in Fig. 1(d) has been arbitrarily set equal to zero before the discharge is initiated at  $t=0$ , the phase shown after  $t=0$  is actually the change in phase due to the plasma,

$$\Delta\theta_m(r,t) = \theta_m(r,t) - \theta_m(r,t < 0). \quad (10)$$

From Eq. (6), since by definition  $\theta_1(r,t < 0)$  is zero for all values of  $r$ ,

$$\Delta\theta_m(r,t) = \theta_1(r,t) - [\theta_\tau(r,t) - \theta_\tau(r,t < 0)] + \Delta\theta(r,t). \quad (11)$$

Thus, at the plasma edge where the density is low, collisions do not shorten the lifetime significantly and  $\theta_\tau$  is approximately constant. Thus, for the data shown in Fig. 1(d),

$$\Delta\theta_m(r,t) = \theta_1(r,t) + \Delta\theta(r,t). \quad (12)$$

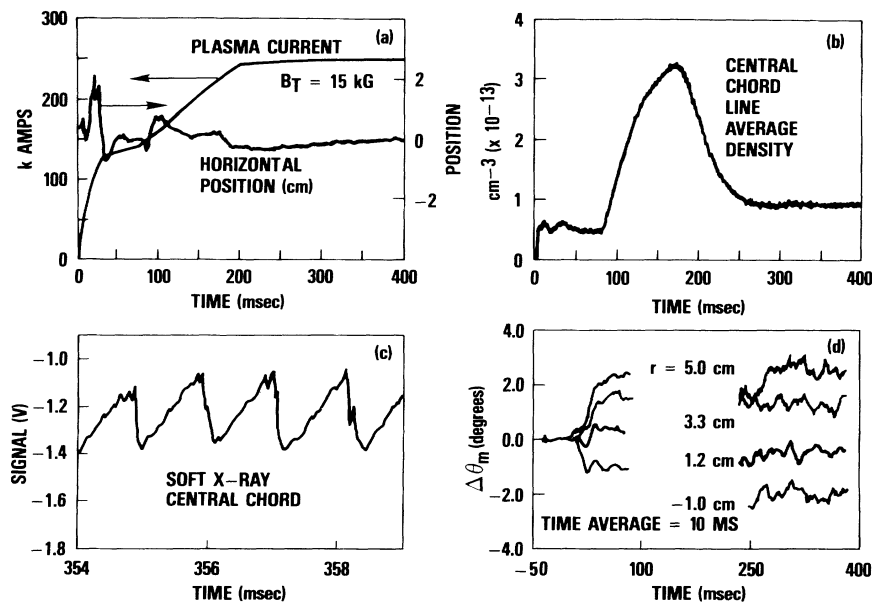


FIG. 1. Typical discharge parameters for the low- $q_a$  discharge discussed here. Shown in (d) are the measured angles,  $\Delta\theta_m$ , as functions of time at four geometric radial positions. These data have been averaged over 10 ms and over twenty shots. The lack of data between 100 and 250 ms results from the density increase required to achieve a stable plasma current ramp.

TABLE I. Relevant measurements for determination of  $q_0$  for tokamak discharge parameters shown in Fig. 1. All measured angles are averaged over 50 ms about  $t=350$  ms. The measured  $\Delta\theta_m^+$  represent an average of 21 shots, while  $\Delta\theta_m^-$  represent an average over 14 shots. Statistical errors are shown for the last two columns only.

$r$ (cm)	$\Delta\theta_m^+$ (deg)	$\Delta\theta_m^-$ (deg)	$\tau$ (ns)	$r'$ (cm)	$\theta_1$ (deg)
25.6	7.90	7.85	27	$30.3 \pm 0.2$	$7.9 \pm 0.02$
21.2	8.35	8.59	20	$24.7 \pm 0.2$	$8.5 \pm 0.02$
7.2	3.27	3.80	12	$9.3 \pm 0.5$	$3.5 \pm 0.05$
5.0	1.78	2.41	9	$6.7 \pm 0.6$	$2.1 \pm 0.06$
3.3	0.40	1.09	8	$4.7 \pm 0.6$	$0.7 \pm 0.06$
1.2	-1.61	-0.81	5	$2.0 \pm 0.4$	$-1.2 \pm 0.04$
-1.1	-3.11	-2.45	8	$0.4 \pm 0.7$	$-2.8 \pm 0.07$
-4.7	-6.60	-5.68	1	$-4.4 \pm 1.1$	$-6.1 \pm 0.1$

With use of Eq. (8) this becomes

$$\Delta\theta_m(r, t) = \theta_1(r', t), \quad (13)$$

where  $r' = r + u\tau$ . Thus  $\Delta\theta_m$  at 25.6 cm is actually indicative of the tilt angle,  $\theta_1$ , at 30.3 cm.

Near the central axis  $\theta_r$  is reduced by collisions with electrons and protons, resulting in a significant difference between the measured  $\Delta\theta_m$  and the tilt angle  $\theta_1$ . However, if the direction of polarization rotation is reversed, both  $\theta_1$  and  $\Delta\theta_1$  in Eq. (10) change sign while  $\theta_r$  remains unchanged. Thus, by measurement of  $\Delta\theta_m$  for identical tokamak discharges using both polarization rotation directions, the change in  $\theta_r$  (and  $\tau$ ) can be determined, as well as  $\theta_1$  and the radial correction  $u\tau$ .

The results of the measured phase shifts at several radial positions in TEXT are shown in Table I for a set of similar discharges with the parameters shown in Fig. 1. To obtain adequate Li-beam penetration and minimize collisionally induced fluorescence, the line-average density must be kept below  $\approx 1 \times 10^{13} \text{ cm}^{-3}$ . To obtain sufficiently precise angles, the data must be averaged over time and over several shots. Table I includes the phase shift measured for both polarization rotation directions at each geometric detector position. The derived Li  $2P$  lifetime and the corrected radius are shown, as well as the corrected magnetic field tilt angle. The corrected results for the six channels near the central axis of the torus are plotted in Fig. 2. Also shown is a straight-line fit to the central four points. With use of this fit to determine both the magnetic axis and  $(d\theta_1/dr)_0$ ,  $q_0$  is found to be 0.72 for this discharge. Since the plasma density at the location of these four points is approximately constant (as determined by a six-channel far-infrared interferometer<sup>13</sup>), the corrections to both  $r$  and  $\theta$  are approximately constant, and  $q_0$  can be determined without our applying the corrections as 0.68 and 0.70 for each polarization rotation direction. Normal

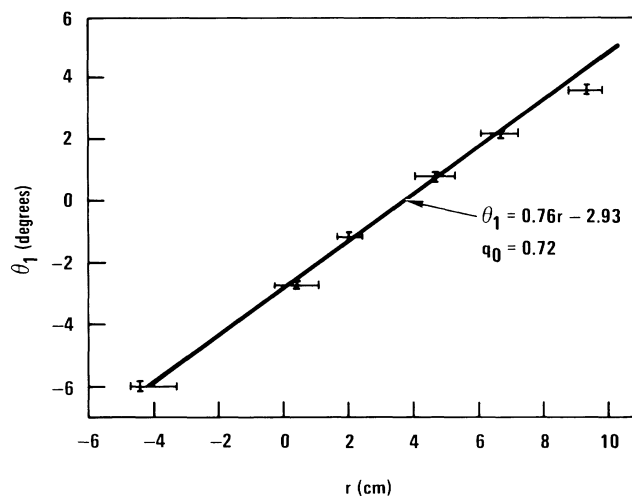


FIG. 2. Measured tilt angles,  $\theta_1$ , near the central axis for discharges similar to that shown in Fig. 1. The straight line is a linear regression fit to the central four points only.

sawtooth oscillations with a 1-ms period and high-frequency precursor oscillations are apparent from the soft x-ray monitor.

A statistical analysis indicates that the largest error contribution for each channel results from the uncertainty in the corrected radial position due to the uncertainty in  $\tau$ . However, as stated above, this systematic error is essentially the same for each of the four central channels and will not contribute significantly to the error in  $q_0$ . An analysis of the uncertainty in  $d\theta/dr$  plus the uncertainty<sup>14</sup> in  $R$  yields an uncertainty of  $\pm 0.05$  in  $q_0$ .

Similar data have been obtained for two other plasma conditions. The results of all three sets of data are summarized in Table II. These results show that as the edge  $q$  is raised  $q_0$  also increases, and when the sawtooth phenomenon is not observed,  $q_0$  is measured to be above 1.0.

In conclusion, we have definitive measurements that demonstrate that  $q_0$ , when averaged over several sawtooth periods, is significantly lower than 1 for low- $q_a$  discharges on the Ohmically heated TEXT. These results are in agreement with previously reported measurements of  $q_0$  which relied on techniques having a significantly less straightforward interpretation. These techniques include far-infrared Faraday rotation,<sup>7</sup> fast

TABLE II. Measured  $q_0$  for several discharge conditions.

$I_p$ (kA)	$B_T$ (T)	$q_a$	$q_0$	Sawtooth period (ms)
240	1.5	2.3	$0.7 \pm 0.05$	1.0
200	2.0	3.4	$0.8 \pm 0.1$	1.0
100	2.0	7.4	$1.1 \pm 0.1$	a

<sup>a</sup>No oscillation observed.

ion orbits,<sup>4,5</sup> and electron-cyclotron-modulated Thomson scattering.<sup>3</sup> Results reported from the ASDEX tokamak<sup>2</sup> based on the Zeeman polarization of lithium are much nearer to 1, but have large error bars in the negative direction because of a limited number of data points near the axis. The nonlinear relaxation of the internal kink, if indeed the relevant instability, does not restrict the time-averaged central  $q$  from falling significantly below unity. However,  $q_0$  does increase with  $q_a$  and becomes greater than 1 for nonsawtooth discharges.

We wish to acknowledge useful discussions with A. Wootton and H. Soltwisch, and the technical aid of the TEXT personnel. This work was supported under Department of Energy Contract No. DE-AC03-84ER53158.

---

<sup>(a)</sup>Permanent address: Institute of Physics, Chinese Academy of Science, Beijing, China.

<sup>1</sup>H. P. Furth, *Plasma Phys. Controlled Fusion* **28**, 1305 (1986).

<sup>2</sup>K. McCormick *et al.*, *Phys. Rev. Lett.* **58**, 491 (1987).

<sup>3</sup>M. J. Forrest, P. G. Carolan, and N. J. Peacock, *Nature (London)* **271**, 718 (1978).

<sup>4</sup>R. J. Goldston, *Phys. Fluids* **21**, 2346 (1978).

<sup>5</sup>D. D. Meyerhofer, R. J. Goldston, R. Kaita, and D. L. Herndoz, *Bull. Am. Phys. Soc.* **27**, 1049 (1982). Note that the technique and apparatus used here were the same as in Ref. 4, but axial  $q$  well below 1 was reported.

<sup>6</sup>G. L. Jahns, M. Soler, B. V. Waddell, J. D. Callen, and H. R. Hicks, *Nucl. Fusion* **18**, 409 (1978), and references therein; G. Bateman, *MHD Instabilities* (MIT Press, Cambridge, MA, 1978).

<sup>7</sup>H. Soltwisch, *Rev. Sci. Instrum.* **57**, 1939 (1986).

<sup>8</sup>W. Pfeiffer, F. B. Marcus, C. J. Armentrout, G. L. Jahns, T. W. Petrie, and R. E. Stockdate, *Nucl. Fusion* **25**, 655 (1985).

<sup>9</sup>K. W. Gentle, *Nucl. Technol. Fusion* **1**, 479 (1981).

<sup>10</sup>W. P. West, *Rev. Sci. Instrum.* **57**, 2006 (1986).

<sup>11</sup>W. P. West and D. M. Thomas, *Rev. Sci. Instrum.* **57**, 1843 (1986).

<sup>12</sup>W. P. West, D. M. Thomas, E. S. Ensberg, J. S. deGrassie, and F. F. Baur, *Rev. Sci. Instrum.* **57**, 1552 (1986).

<sup>13</sup>B. Richards, private communication.

<sup>14</sup>P. R. Bevington, *Data Reduction and Error Analysis for the Physical Sciences* (McGraw-Hill, New York, 1969).